Linear theory of uncompensated thermal blooming in turbulence

D. H. Chambers, T. J. Karr, J. R. Morris, P. Cramer, and J. A. Viecelli
Lawrence Livermore National Laboratory, P.O. Box 808, L-495, Livermore, California 94550

A. K. Gautesen
Department of Mathematics, Iowa State University, Ames, Iowa 50011
(Received 24 April 1989; revised manuscript received 12 February 1990)

A linearized theory of small perturbations in thermal blooming gives a surprisingly accurate description of the initial evolution of a plane wave propagating through an absorbing fluid medium. In the case of constant absorption and fluid velocity, a sinusoidal perturbation of the optical field grows quasiexponentially at a rate determined by its Fresnel number and the accumulated optical-path difference due to blooming. Perturbations with small transverse length scales grow more rapidly than those with large length scales. The evolution of the optical field and spectrum in the presence of optical turbulence is accurately described. The growth of the small-scale fluctuations eventually leads to a decrease in plane-wave amplitude. This growth puts an ultimate limit on the amount of power that can be propagated through a turbulent medium such as the atmosphere. More complicated cases with varying absorption and velocity profiles can be analyzed using a WKB approximation. Numerical simulations show growth suppression when the velocity varies along the optical path. These predictions from the linearized theory agree well with results from numerical simulations of the full nonlinear system and thus provides a standard for comparing different numerical codes.

INTRODUCTION

A laser beam propagating through a weakly absorbing fluid medium heats the fluid, changing the local density. This causes variations in refractive index, which result in phase and irradiance fluctuations of the beam field. For low-power lasers these fluctuations do not significantly affect the propagation of the beam. However, as the power is increased, these self-induced refractive-index changes can degrade the ability to focus or aim the beam. The details of this self-induced distortion, known as thermal blooming, depend on the irradiance and diameter of the beam and the magnitude of the temperature change.

For high-irradiance, small-diameter beams, the initial irradiance distribution and edge effects dominate, leading to large distortions on the scale of the whole beam. These whole-beam effects have been extensively studied both analytically and numerically by many researchers (see Walsh and Ulrich[1]). In particular, perturbative whole-beam solutions for homogeneous media have been obtained by Gautesen and Morris.[2]

For larger-diameter beams, irradiance changes induced by whole-beam blooming are less, and small-scale irradiance scintillations from inhomogeneities in the medium become important. The blooming intensifies these inhomogeneities in a process called stimulated thermal Rayleigh scattering (STRS).[3] This phenomenon occurs for collimated beams with large Fresnel numbers N_F when the total amount of phase distortion from whole-beam blooming remains much less than N_F. The Fresnel number $N_F=\pi D^2/4\lambda L$ is proportional to the ratio between the length at which diffraction becomes important for the whole beam D^2/λ to the total path length L, where D is the diameter of the beam and λ is the wavelength. Small-scale distortion is also important when adaptive-optics systems are used to correct for turbulence and whole-beam blooming. These systems generally correct only large-scale distortions, leaving the smaller-scale scintillations unaffected. The growth of these uncorrected small-scale scintillations puts an ultimate limit on the amount of power that can be propagated by an adaptive system through a turbulent medium such as the atmosphere. The magnitude of the growth depends on laser wavelength and path length through the Fresnel number of the small-scale perturbations $N_p=\pi\Lambda^2/4\lambda L$, where Λ is the length scale of the perturbation. Growth is small for large Fresnel numbers ($N_p \gg 1$) and large for small Fresnel numbers ($N_p \ll 1$). This effect has been observed by Karr *et al.*[4] in the propagation of an argon laser (1–3 W, 2–5-mm diameter) through a 1.2-m cell of CCL_4 scaled to reproduce typical atmospheric Fresnel numbers.

Analytical results for small scale thermal blooming are extremely difficult to obtain due to the nonlinear coupling between the induced refractive index variations and the beam field. This makes a numerical approach necessary for most problems of practical interest. However, in this paper analytical results based on linearization around a known solution are shown to describe much of the phenomenology of thermal blooming in turbulent media when whole beam effects are small. Small-scale phase and amplitude perturbations are found to grow quasiexponentially in a fluid medium with constant absorption in agreement with previous results.[5–9] In addition, the evo-

lution of the optical spectrum is obtained for propagation through an optically turbulent absorbing fluid. The linearized theory agrees well with numerical solutions of the full nonlinear equations, accurately predicting the evolution of phase and amplitude fluctuations up to saturation.

LINEAR THEORY OF THERMAL BLOOMING

The optical field in thermal blooming is described by the paraxial wave equation

$$2ik\frac{\partial E}{\partial z}=\nabla^2 E+2k^2(n-1)E,\quad \nabla^2=\frac{\partial^2}{\partial x^2}+\frac{\partial^2}{\partial y^2}\ , \tag{1}$$

where E is the electric field amplitude and n is the ratio of the actual refractive index field to the constant background refractive index. This ratio is assumed to vary little from unity so that the approximation $n^2-1\approx 2(n-1)$ in the paraxial equation is valid. The beam propagates in the $+z$ direction with a wave number $k=2\pi/\lambda$, where λ is the wavelength in the medium. The refractive index field is described by the hydrodynamic equation for a passive contaminant in a fluid,

$$\frac{\partial n}{\partial t}+(\mathbf{u}\cdot\nabla)n=-CI+d\nabla^2 n \tag{2}$$

where $I=|E|^2$ is the optical irradiance, d is the diffusivity, $\mathbf{u}(z)$ is the mean transverse fluid velocity, and $C(z)$ is a material parameter proportional to the absorption coefficient of the fluid $\alpha(z)$, $C=(\partial n/\partial\rho)\alpha\beta_T/C_p$. These governing equations are valid for weakly absorbing mediums such as the atmosphere where density changes are too small for buoyancy to affect the velocity field (heated parcels of fluid are convected out of the beam before buoyancy can significantly change their velocity).

Equations (1) and (2) are separately linear equations for E and n. The coupling terms, though, are nonlinear, making analysis of the full system extremely difficult. However, one can calculate the behavior of small perturbations away from some nominal solution using linear analysis.[10] Consider the case of small perturbations from the solution for a plane wave $E=E_0+E_1$, where E_0 is the plane-wave solution and E_1 is a perturbation $|E_1|\ll E_0$. The irradiance in the plane-wave solution remains constant $I_0=E_0^2$. In terms of irradiance and phase the full electric field (plane wave plus perturbation) can be written

$$E=\sqrt{I_0(1+F)}e^{-i(\phi_0+\phi)}\ , \tag{3}$$

where F is the irradiance perturbation and ϕ is the phase perturbation. Substituting this into the governing equations and retaining only the terms linear in F and ϕ gives

$$\frac{\partial F}{\partial z}=-\frac{1}{k}\nabla^2\phi\ , \tag{4a}$$

$$\frac{\partial\phi}{\partial z}=k\left[\mu+\frac{1}{4k^2}\nabla^2 F\right]\ , \tag{4b}$$

$$\frac{\partial\mu}{\partial t}+(\mathbf{u}\cdot\nabla)\mu=-\Gamma F+d\nabla^2\mu\ , \tag{5}$$

where $\Gamma=CI_0$ and $\mu=n-1$ is the refractive-index perturbation associated with the field perturbation. These equations determine the growth (or decay) of the perturbation as a function of z and t.

Equations (4) and (5) are solved given initial perturbations in the optical fields F and ϕ, and/or perturbations in the refractive index field μ. The equations are Fourier transformed in the transverse xy plane, then Laplace transformed in time to obtain

$$\frac{\partial\hat{F}_\kappa}{\partial z}=\frac{\kappa^2}{k}\hat{\phi}_\kappa\ , \tag{6a}$$

$$\frac{\partial\hat{\phi}_\kappa}{\partial z}=k\left[\hat{\mu}_\kappa-\frac{\kappa^2}{4k^2}\right]\hat{F}_\kappa \tag{6b}$$

$$\nu\hat{\mu}_\kappa+i(\boldsymbol{\kappa}\cdot\mathbf{u})\hat{\mu}_\kappa=-\Gamma\hat{F}_\kappa-d\kappa^2\hat{\mu}_\kappa+\mu_\kappa^0 \tag{7}$$

where κ is the transverse wave vector, ν is the conjugate Laplace variable for time, and μ_κ^0 is the initial perturbation of the refractive-index field. In atmospheric propagation μ_κ^0 represents the natural turbulent fluctuations of refractive index. The κ subscript indicates the Fourier transform while the caret indicates the Laplace transform. These equations can be combined to obtain a single equation for F_κ:

$$\frac{d^2\hat{F}_\kappa}{dz^2}+a_\kappa^2\beta^2(\bar{\nu})\hat{F}_\kappa=\frac{\kappa^2\mu_\kappa^0}{\bar{\nu}}\ , \tag{8}$$

where

$$\beta^2(\bar{\nu})=1+\frac{2k\Gamma}{a_\kappa\bar{\nu}}\ ,$$

$$\bar{\nu}(z)=\nu+d\kappa^2+i[\boldsymbol{\kappa}\cdot\mathbf{u}(z)]\ ,$$

and $a_\kappa=\kappa^2/2k$. Let $\hat{J}_\kappa(z)$ be the solution of (8) for the special case of $\mu_\kappa^0=0$, $F_\kappa(0)=0$, and $F_\kappa'(0)=1$, where $F_\kappa'=dF_\kappa/dz$. The solution to (8) for general initial conditions $\hat{F}_{\kappa 0}$ and $\hat{\phi}_{\kappa 0}$ at $z=0$ can be written in terms of $\hat{J}_\kappa(z)$ and the function $\hat{K}_\kappa(z,z')=J_\kappa(z,z')/\bar{\nu}(z')$, where $J_\kappa(z,z')$ is the Green's function for (8) (Ref. 11):

$$\hat{F}_\kappa(z)=\hat{J}_\kappa'(z)\hat{F}_{\kappa 0}+2a_\kappa\hat{J}_\kappa(z)\hat{\phi}_{\kappa 0}+\kappa^2\int_0^z K_\kappa(z,z')\mu_\kappa^0(z')dz'\ . \tag{9}$$

The solution for the phase fluctuation $\hat{\phi}_\kappa$ can be obtained from (9) using (6a). Note that the function $\hat{K}_\kappa$ is independent of the turbulent refractive-index fluctuations.

The function K_κ can be written in closed form for only a few cases of absorption $\Gamma(z)$ and mean velocity profile $\mathbf{u}(z)$. The problem can be simplified somewhat by noting that the diffusion term $d\kappa^2$ in $\bar{\nu}$ represents a multiplicative factor of $\exp(-d\kappa^2 t)$ in the expression for $K_\kappa(z,z',t)$, i.e., if $K_\kappa(z,z',t)$ is calculated for $d=0$, it is $K_\kappa(z,z',t)\exp(-d\kappa^2 t)$ for nonzero d. If $\mathbf{u}(z)$ is constant, the problem can be simplified further by rewriting the equations in terms of the retarded time $t-\mathbf{x}\cdot\mathbf{u}/u^2$, eliminating the term $i\boldsymbol{\kappa}\cdot\mathbf{u}$ from $\bar{\nu}$ so that $\bar{\nu}=\nu$. However these simplifications still do not allow closed form expressions for K_κ for general absorption profiles $\Gamma(z)$. In a later section, a method of obtaining approximate solu-

tions to (9) for general absorption and velocity profiles is presented.

UNIFORM MEDIUM

For constant absorption and constant velocity, the integral in (9) becomes a convolution with $K_\kappa(z,z',t)=K_\kappa(z-z',t)$. A simple analytic form for $K_\kappa(z,t)$ can be derived for this case:

$$K(z,t)=\sum_{n=0}^{\infty}\frac{(-\Gamma tkz)^n}{(n!)^2}[zj_n(a_\kappa z)]\ , \tag{10}$$

$$\hat{K}(z,\nu)=\frac{\sin(a_\kappa\beta z)}{\nu a_\kappa\beta}\ , \tag{11}$$

where t is the retarded time in the convected frame, $j_n(x)$ are spherical Bessel functions, and $\Gamma tkz=2\pi N_\lambda$ is the phase shift in radians caused by thermal blooming. The κ subscripts have been dropped with the understanding that all subsequent analysis will be in the Fourier domain. This expression for a uniformly absorbing medium was first derived by Glass.[12] The form of (10) makes it difficult to determine at first glance whether the initial perturbation will grow or decay in time under the influence of thermal blooming. This question is critical in determining the degradation of a laser beam propagating through the medium.

The rate of phase-shift accumulation at a constant altitude for a typical case of high-energy atmospheric propagation is several to tens of waves per second. For example, a 1-μm-wavelength laser with an absorbed power of 10^{-5} W/cm^3 accumulates phase change at a rate of 10 waves per second for zero wind after propagating 1 km. For constant nonzero wind, the phase change accumulates as a parcel of air is convected across the beam. The rate of phase accumulation for a constant wind of 1 m/s in the previous example is 10 waves per meter. The total distortion at the downwind edge of the beam is proportional to the beam diameter and its duration.

The method of steepest descents can be used to evaluate the Laplace inversion integral of (11) for large time t. The results for two different limits are

$$K(z,t)\sim\frac{z}{\pi^2\sqrt{12N_\lambda/N_p}}\exp\left[\frac{3\pi}{2}\left[\frac{N_\lambda}{4N_p}\right]^{1/3}\right]\times\sin\left[\frac{3\sqrt{3}}{2}\left[\frac{N_\lambda}{4N_p}\right]^{1/3}\right] \tag{12}$$

for $N_p^2N_\lambda\gg1$ with $N_\lambda\gg N_p$, and

$$K(z,t)\sim\frac{k/\sqrt{\pi}}{\kappa^2(2\pi N_\lambda)^{1/4}}e^{\sqrt{4\pi N_\lambda}}\sin\left[\frac{\pi^2}{4N_p}+\sqrt{4\pi N_\lambda}-\frac{\pi}{8}\right] \tag{13}$$

for $N_p^2N_\lambda\ll1$ with $N_\lambda>1$, where $N_p=\pi^2k/2\kappa^2z$ is the Fresnel number for perturbations with transverse wave number κ. These asymptotic limits were first obtained by Glass[12] and Briggs[9] using different methods. They show that perturbations in the linearized theory grow without bound for increasing N_λ. The first result (12) is applicable for perturbations with large Fresnel numbers (large spatial scales) while the second result (13) applies to small Fresnel numbers (small spatial scales). These approximations appear to work well for N_λ of order 1 and greater. The result for small spatial scales remains valid even for N_λ less than one (see Fig. 5). The growth of the smaller scale perturbations is faster than the growth of the larger scales and independent of Fresnel number. However, for much larger N_λ the growth rate of the small scales should approach that given by (12). This is reflected in the upper bound for $K(z,t)$ (see the Appendix):

$$|K(z,t)\le 9z\left[\frac{N_p}{N_\lambda}\right]^{1/3}\exp\left[\frac{3\pi}{2}\left[\frac{N_\lambda}{4N_p}\right]^{1/3}\right]\ ,$$

$$\frac{N_\lambda}{N_p}\ge\frac{2}{\pi^3}\ . \tag{14}$$

Eventually the amplitude fluctuations become so large that the linearized analysis in invalid and the growth levels off. This regime of growth saturation with large fluctuations is not of much practical interest, however, since the quality of the beam is poor.

Physically, the growth of the perturbation can be understood as a self-stimulating scattering process. Initial phase perturbations in the beam are converted into irradiance fluctuations one Fresnel length down the propagation path. Absorption results in differential heating and refractive-index fluctuations which cause more scattering and phase fluctuations. At large scattering angles this process has long been known as stimulated thermal Rayleigh scattering.[3] Roughly speaking, the beam writes its own diffraction grating into the medium. For small-scale perturbations the plane wave diffracts off the perturbations. Interference between the diffracted wave and the plane wave creates a more intense heating pattern further down the propagation path. The second heating pattern is opposite to the original perturbation so that spots which were initially hotter than average propagate to spots which are cooler than average. However, the magnitude of the temperature difference increases as the beam propagates, leading to oscillatory growth of the perturbations (Fig. 1). The rate of growth depends upon the coherence of the scattering patterns. The highest growth rates occur when the heating patterns burned into the fluid remain strictly aligned along the propagation axis, i.e., a uniform velocity field. Variations in fluid velocity along the z direction disrupt this alignment and can reduce the growth rates.

For perturbations with large spatial scales $a_\kappa z\ll1$ the process can be described in terms of geometric optics as an alternating focusing and defocusing of the perturbations. Any small perturbation that tends to focus a part of the beam causes a hot spot to form some distance down the geometric ray through the perturbation. This hot spot creates a local-density minimum which acts as a divergent lens which produces a cool spot further down the path. The cool spot focuses the beam again into another hot spot. As in the diffractive case the resulting focusing and defocusing is unstable, causing unbounded oscillatory growth of the perturbations.

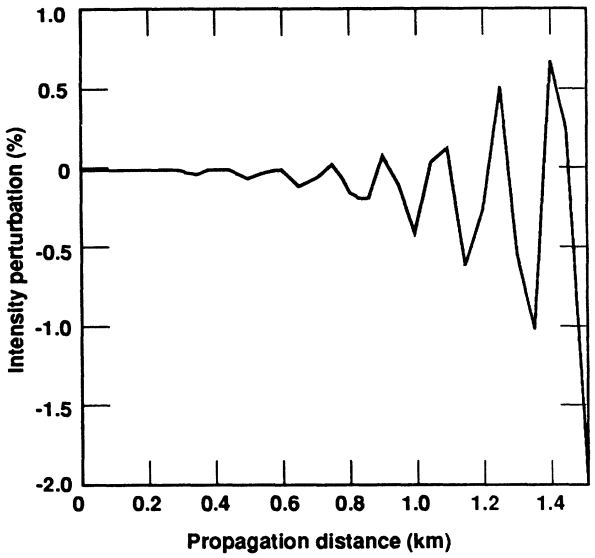

FIG. 1. FOURD calculation of oscillatory growth of intensity perturbation for a 2-m-wide infinite slit beam ($\lambda=1\mu$m) propagating through a uniform atmosphere with constant wind of 2.63 m/s perpendicular to the slit. Initial intensity perturbation was 0.001% with a period of 1 cm. Blooming rate was 5.7 waves per kilometer, or 7.5 waves per second at 1 km.

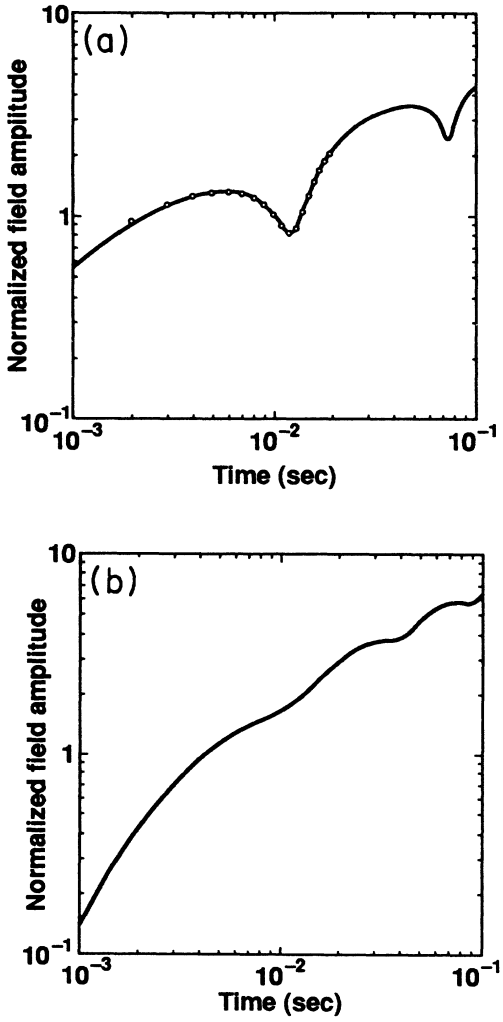

FIG. 2. Growth from a small initial sinusoidal log-amplitude fluctuation. Solid line is linear theory, symbols are ORACLE results. Blooming rate was 112.8 waves per second. (a) $N_p=3$, (b) $N_p=0.39$.

The linearized theory was tested against the results from ORACLE, a numerical code for thermal blooming developed by Viecelli[13] at Lawrence Livermore National Laboratory. ORACLE solves the full nonlinear-propagation problem [Eqs. (1) and (2)] on a discrete four-dimensional mesh in which the fluid medium is represented by discrete layers. The fluid density field is a set of two-dimensional real arrays, one for each layer. The electric field is a single two-dimensional complex array which propagates through the density arrays. Turbulence is represented by using random phase screens with Kolmogorov spectra to initialize the density arrays.[14] For each time step ORACLE propagates the electric field forward using a split-operator Fourier method. It then convects the density arrays for one time step, calculates the heating, and repeats the cycle. The density arrays are convected by multiplying their Fourier transforms by a complex phase factor. Specifically, the computational domain consisted of multiple square meshes spaced evenly in the direction of propagation ($+z$). The mesh resolution varied from 32×32 for Figs. 2 and 10 to 128×128 for Figs. 7 and 8. The number of z steps varied from 40 for the large mesh to 400 for the smaller mesh. The solutions obtained using the Fourier method are periodic in planes transverse to the propagation direction, with periods equal to the mesh width. ORACLE is closely related to the thermal-blooming code FOURD used by Fleck, Morris, and Feit.[14]

Comparisons between numerical simulations and linear theory were made for two cases of interest: constant initial conditions with no index fluctuations, and zero initial conditions with index fluctuations corresponding to atmospheric turbulence. The first case demonstrates the validity of the linear theory and the asymptotic forms of $K(z,t)$ for large time. The second demonstrates the ability of the linear theory to predict the amplification of turbulent index fluctuations for a physically interesting case. Agreement between numerical simulation and theory is found to be an important criterion for determining the validity of any numerical code for thermal blooming.

Consider the case where the electric field at $z=0$ has a sinusoidal perturbation with constant amplitude and spatial wave number κ. The initial conditions in (9) are $F_{\kappa 0}=2\chi_0/\nu$ and $\phi_{\kappa 0}=\phi_0/\nu$, where χ_0 and ϕ_0 are the log-amplitude and phase of the Fourier transform of the perturbation. The solution for the Fourier-transformed log-amplitude $\chi(z,t)$ and phase $\phi(z,t)$ are obtained from (6a) and (9):

$$\chi(z,t)=K'(z,t)\chi_0+a_\kappa K(z,t)\phi_0 , \tag{15}$$

$$\phi(z,t)=\frac{1}{a_\kappa}K''(z,t)\chi_0+K'(z,t)\phi_0 , \tag{16}$$

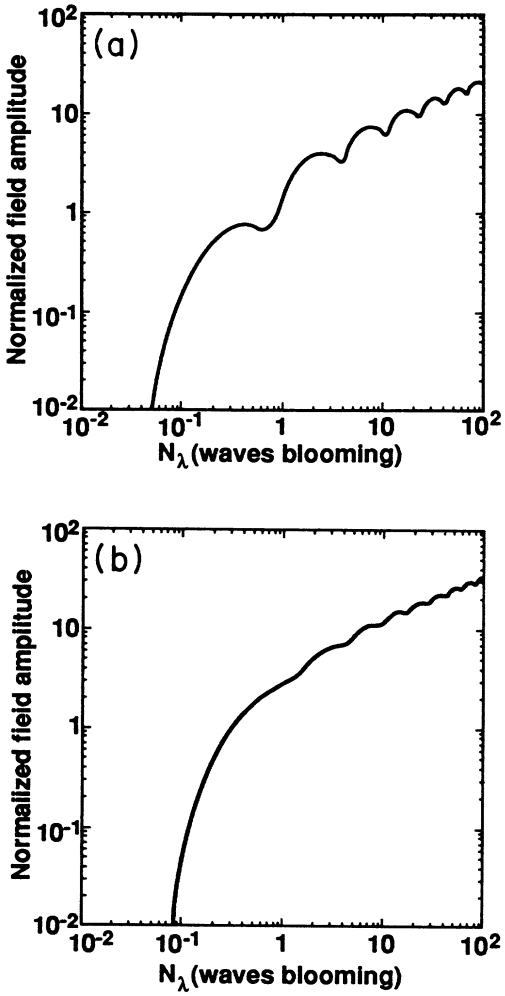

FIG. 3. Growth from a small initial sinusoidal phase fluctuation from linear theory. (a) $N_p=3$, (b) $N_p=0.39$.

where the log-amplitude $\chi(z,t)=F(z,t)/2$. From these the normalized electric field magnitude of the perturbation is

$$\frac{|E_\kappa(z,t)|^2}{I_0}=\chi^2(z,t)+\phi^2(z,t)\ . \tag{17}$$

This expression can be calculated using the exact series representation or the large-time asymptotic expressions for $K(z,t)$. The exact series result is shown in Figs. 2 and 3 along with numerical results for the full nonlinear problem from ORACLE. Phase and log-amplitude perturbations are considered separately.

In both phase and log-amplitude perturbations, the electric field magnitude generally increases with time. Oscillations of the magnitude are present in both cases but are larger for phase perturbations. Both the full series representation and the asymptotic expression reflect this behavior. For large spatial scales (large Fresnel number) the oscillations can be so great that the perturbed field is smaller than the initial field in certain intervals of time. This could cause wide disagreement between numerical simulations which differ only slightly in their initial parameters. A range of Fresnel numbers and time intervals must be investigated to establish the overall growth of perturbations in the field. In the case of ORACLE, the agreement between ORACLE results and linear theory confirms the accuracy of the numerical code. Thus linear STRS theory provides the first opportunity for independent confirmation of numerical models of small-scale thermal blooming.

AMPLIFICATION OF OPTICAL TURBULENCE

The interaction between thermal blooming and a random field of refractive index fluctuations can be investigated by choosing zero initial conditions in the solution given by (9), i.e., $F_{\kappa 0}=0$ and $\phi_{\kappa 0}=0$. For this case the log-amplitude and phase are

$$\chi(z,t)=a_\kappa k\int_0^z K(z-s,t)\mu_\kappa^0(s)ds\ , \tag{18a}$$

$$\phi(z,t)=k\int_0^z K'(z-s,t)\mu_\kappa^0(s)ds\ . \tag{18b}$$

Since the refractive index is a random field, appropriate measures of the optical field are the spectra of the log-amplitude and phase:

$$\langle\chi\chi^*(z,t)\rangle=a_\kappa^2k^2\int\int_0^z K(z-s,t)K(z-s',t)\times\langle\mu_\kappa^0(s)\mu_{\kappa_0}(s')\rangle ds\,ds'\ , \tag{19a}$$

$$\langle\phi\phi^*(z,t)\rangle=k^2\int\int_0^z K'(z-s,t)K'(z-s',t)\times\langle\mu_\kappa^0(s)\mu_\kappa^0(s')\rangle ds\,ds\ , \tag{19b}$$

where the brackets $\langle\ \rangle$ indicate an ensemble average over realizations of the field μ_κ^0. For the special case of atmospheric optical turbulence, the index fluctuations have a Kolmogorov spectrum with an amplitude characterized by the structure constant $C_n^2(z)$, which is generally a function of position along the optical path. Following Tatarski,[15] the log-amplitude and phase spectra are given by

$$\langle\chi\chi^*\rangle=\frac{0.207}{\kappa^{11/3}}a_\kappa^2k^2\int_0^z C_n^2(s)K^2(z-s,t)ds\ , \tag{20a}$$

$$\langle\phi\phi^*\rangle=\frac{0.207}{\kappa^{11/3}}k^2\int_0^z C_n^2(s)K'^2(z-s,t)ds\ , \tag{20b}$$

where 0.207 is the approximate numerical value of $5/[9\Gamma(1/3)]$. Their sum in the linearized theory gives the spectrum Φ of the electric field perturbation as a function of the transverse wave vector κ, the propagation distance z, and the retarded time t. (The sum of the variances does not give Φ when the linearized theory breaks down.) Substituting the series expansion (10) for $K(z,t)$ into the sum gives a power series in radians of blooming $\theta=2\pi N_\lambda$ with coefficients proportional to integrals of products of spherical Bessel functions. These integrals can be evaluated in closed form as sums over products of spherical Bessel functions.[16] The result is

$$\Phi(l,\theta)=\frac{0.0243z}{kN_T^{5/6}l^{11/6}}\left\{1-\frac{\theta}{l}\left[1-\frac{\sin(2l)}{2l}\right]\right.$$
$$+\sum_{n=2}^{\infty}\frac{(-\theta)^n}{n!(n+1)!}\left[2^n[lj_n(l)\sin l-h_n(l)\cos l]\right.$$
$$\left.\left.+(n+1)l\sum_{m=0}^{M_n}\binom{n}{m}\binom{n}{m+1}a_m(n-1)[h_m(l)j_{n-m-1}(l)-j_m(l)h_{n-m-1}(l)]\right]\right\}, \quad (21)$$

where $l=a_\kappa z=\pi^2/4N_p$, $h_n(l)=nj_n(l)-lj_{n-1}(l)$, $\binom{n}{m}$ are the binominal coefficients, M_n is the integer part of $n/2-1$, $N_T=\pi r_0^2/4\lambda z$ is the Fresnel number of the optical turbulence with coherence length[17] r_0, and $a_m(n)$ are numerical coefficients given by

$$a_m(n)=\int_0^1[(1-t)^m(1+t)^{n-m}-(1-t)^{n-m}(1+t)^n]dt$$

The series converges slowly, requiring over 20 terms to obtain convergence for $N_\lambda=5$. The resulting spectrum is shown in Fig. 4 for $N_\lambda=0$ to $N_\lambda=10$. The low-wave-number end of the spectrum is initially damped before starting to grow while the high-wave-number end grows exponentially from the start. For large l the series can be summed explicitly to obtain the asymptotic result

$$\frac{\Phi(l,\theta)}{\Phi(l,0)}\sim\left[1-\frac{\theta}{l}\right]\mathrm{Re}\left[\frac{e^{-i\pi/4}}{\sqrt{\theta}}I_1(2\theta^{1/2}e^{i\pi/4})\times I_0(2\theta^{1/2}e^{-i\pi/4})\right]. \quad (22)$$

The growth rate of the spectrum in the range of $N_p^{-1}>6$ is independent of the Fresnel number and agrees with (22) evaluated in the limit of large θ:

$$\frac{\Phi(l,\theta)}{\Phi(l,0)}\sim\frac{e^{\sqrt{8\theta}}}{4\pi\theta\sqrt{2}}\left[1-\frac{\theta}{l}\right]. \quad (23)$$

The exponential factor in (23) is the square of the exponential factor in (13), the asymptotic form for $K(z,t)$ when $N_p^2N_\lambda\ll1$, $N_\lambda>1$. A comparison between the full series and the asymptotic expression shows that the asymptotic result becomes valid for large wave numbers for $N_\lambda>0.2$ (see Fig. 5).

The wave structure function[17] (Fig. 6) can be calculated from (21) using

$$D(\alpha)=\frac{4\pi k}{z}\int_0^\infty\Phi(l,\theta)[1-J_0(\alpha\sqrt{l})]dl, \quad (24)$$

where α is a nondimensional length related to the separation distance r by $\alpha=r\sqrt{4\pi/\lambda z}$. The initial $r^{5/3}$ Kolmogorov behavior remains undisturbed for $r\gg\sqrt{\lambda z}$ until the spectrum begins to grow for small wave numbers. For $r\ll\sqrt{\lambda z}$ the structure function retains the $r^{5/3}$ dependence but with an exponentially growing amplitude. Alternatively, the structure function could be written in terms of $(r/R)^{5/3}$ where R continually decreases. However, the temptation to interpret R as Fried's coherence length[17] r_0 must be resisted since the definition of r_0 is specific to atmospheric propagation with no blooming. For $r\sim O(\sqrt{\lambda z})$, the structure function develops a plateau which increases in extent as N_λ increases.

The mutual coherence function[18] is proportional to

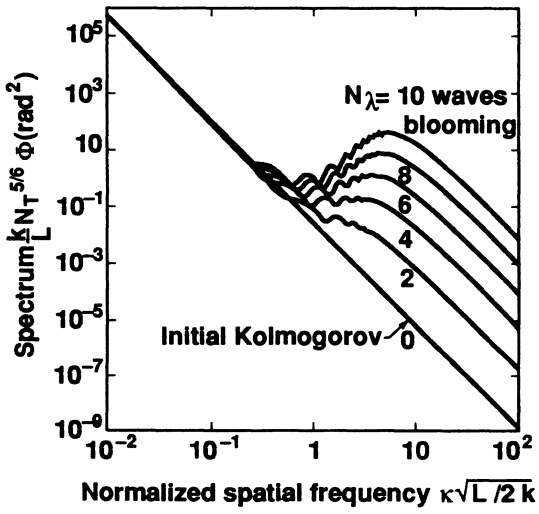

FIG. 4. Evolution of the optical spectrum during thermal blooming with Kolmogorov optical turbulence.

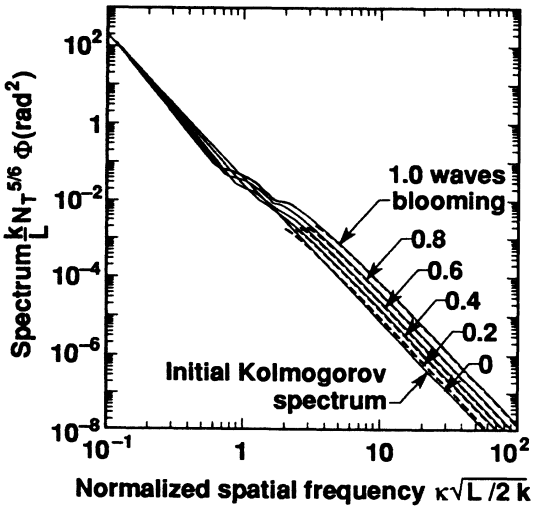

FIG. 5. Initial evolution of the optical spectrum showing agreement between the exact linear analysis (solid line) and the asymptotic expression (dashed line) for high spatial frequencies.

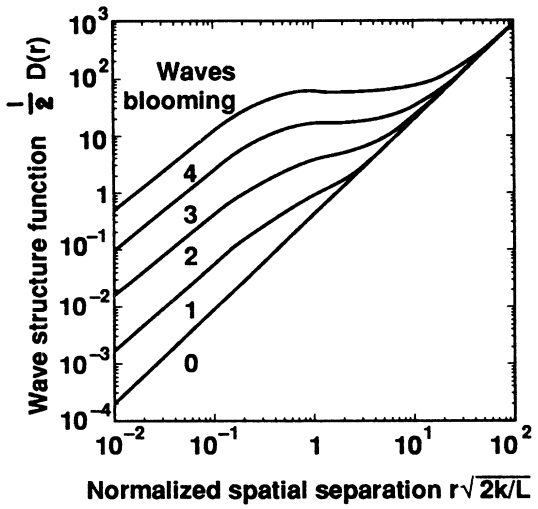

FIG. 6. Evolution of the wave structure function during thermal blooming with Kolmogorov optical turbulence.

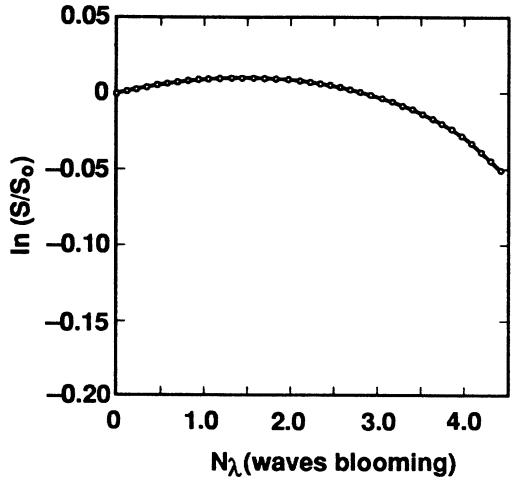

FIG. 7. Evolution of the Strehl ratio with Kolmogorov turbulence ($N_T=785$). Linear analysis (solid line) agrees with ORACLE results (symbols). ORACLE points are ensemble averages over 20 turbulence realizations.

exp[$-D(\alpha)/2$] for propagation through turbulence with no blooming. This result also holds for the linearized theory of thermal blooming since the phase and log-amplitude fields remain Gaussian when the initial refractive-index field is Gaussian. The applicability of this result at later times when the fields evolve nonlinearly is problematic. The crucial question is whether the fields remain Gaussian in this nonlinear regime; nothing conclusive is known about it.

The Strehl ratio will be defined as the ratio of the mean-square amplitude of the plane wave component of the spectrum ($\kappa=0$) at a fixed distance L along the propagation path to the initial value of this component at $z=0$. The initial ($t=0$) value of the Strehl depends on the Fresnel number of the optical turbulence for $z=L$. The evolution of the Strehl with increasing t, however, is given by the integral of the spectrum (21) over all wave vectors excluding $\kappa=0$, and is independent of N_T. This is seen in the Strehls calculated from the numerical simulation shown in Fig. 7. The Strehl increases initially due to the suppression of the low-wave-number end of the spectrum. It then falls rapidly due to the exponential growth of the high wave numbers in the spectrum. After the point at which the Strehl falls off the linearized analysis is suspect since the perturbations are no longer small compared with the plane wave.

The spectrum from the linearized analysis is compared with the result from ORACLE in Fig. 8. The substantial agreement between the two verifies the accuracy of the numerical code and the applicability of linearized analysis to the problem. The exponential growth of the spectrum leads inevitably to the breakdown of the linearized theory. Numerical results for longer times show that the linearized theory generally holds out to the point at which the Strehl begins to fall off. After this point the linearized analysis will eventually break down and nonlinear effects will become evident. Figure 9 shows one case for which the linear analysis disagrees quantitatively with the fully nonlinear numerical simulation. In this example the initial turbulence was quite strong, and the optical fluctuations were saturated at $t=0$. The growth of the high wave numbers in the spectrum is less than the linear prediction and can be attributed to nonlinear saturation effects. Note however that the form of the spectrum is in qualitative agreement with the linear theory.

NONUNIFORM MEDIUM

In the previous section the absorption and velocity of the medium were considered to be constants. Consider

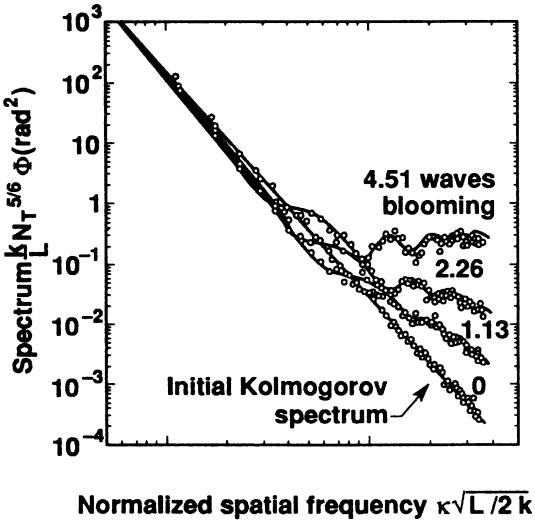

FIG. 8. Comparison of ORACLE results (symbols) with the exact linear analysis for the evolution of the optical spectrum ($N_T=19{,}600$). ORACLE points represent averages over 20 realizations of turbulence.

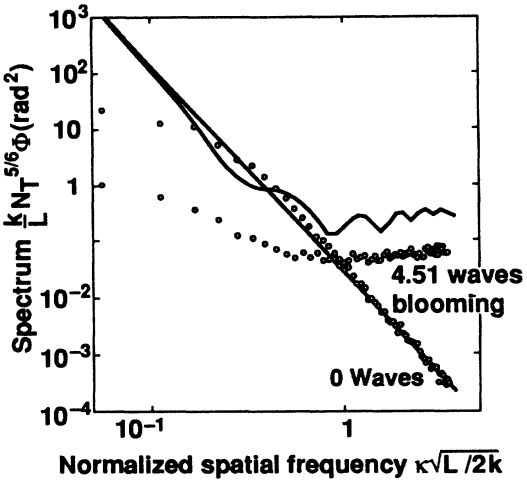

FIG. 9. Comparison of ORACLE results (symbols) with the exact linear analysis for large turbulent fluctuations ($N_T=7.85$). Note the nonlinear saturation of the high frequency end of the spectrum. Linear analysis agrees qualitatively with numerical result. ORACLE points are ensemble averages over 20 turbulence realizations.

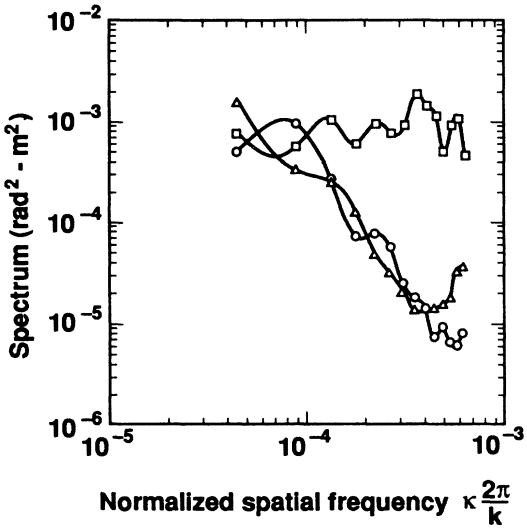

FIG. 10. Time averaged intensity spectra along the κ_y axis ($\kappa_x=0$) for single ORACLE realizations with linear velocity profiles in the y direction. Curves are for $N_T=0.785$ and shear parameters of $S=0$ (□), $S=0.866$ (○), and $S=1.77$ (△). Time averaging was over the interval from 4.5 to 9 waves of blooming. Shearing suppresses the growth for wave vectors parallel to the shear. The growth of the intensity spectrum along the κ_x axis is unaffected.

now the more general case in which the absorption and velocity can vary along the direction of the beam, i.e. $\Gamma=\Gamma(z)$, $\mathbf{u}=\mathbf{u}(z)$. The quantity β^2 in Eq. (8) for the field $F(z)$ becomes a function of z and no general solution exists. However for $|(d\beta/dz)/a_\kappa\beta^2| \ll 1$, a WKB approximation to the function $J(z)$ can be obtained:[10]

$$\hat{J}(z)\approx\frac{1}{a_\kappa\sqrt{\beta(0)\beta(z)}}\sin\left[a_\kappa\int_0^z\beta(z')dz'\right]. \quad (25)$$

The WKB approximation would generally be valid in the cases of strong blooming or medium to high spatial frequencies.

Consider the case where the absorption is constant but the magnitude of the fluid velocity varies linearly with z. The shearing by the velocity profile misaligns the heating patterns created by absorption and reduces the growth rate of the perturbations. Perturbations with transverse wave vectors κ perpendicular to the velocity direction are not affected by the shear since their heating patterns are linear stripes of alternating hot and cold regions aligned with the velocity. For perturbations with wave vectors parallel to the velocity the heated stripes lie transverse to the velocity vectors. Velocity differences between fluid layers cause stripes which were initially aligned in the z direction to become shifted relative to one another. The growth rates for these perturbations are strongly affected by the shear. The time needed to shift the heating patterns between two layers a distance of one Fresnel zone $2\sqrt{\lambda z/\pi}$ is $t_s(z)=2\sqrt{(\lambda z/\pi)}/\Delta v(z)$, $\Delta v(z)=v(z)-v(0)$. The number of waves of blooming accumulated during this time is $N_\lambda(t_s)=\Gamma t_s kz/2\pi$. The inverse of $N_\lambda(t_s)$ is the ratio of shearing rate to blooming rate S. If S is much greater than 1, the shearing is stronger than the blooming and growth suppression can occur.

Equation (25) gives an approximation to the Laplace transform of the blooming function $J(z)$ for the case of linear shear. However, obtaining estimates of growth rates from $J(z)$ is itself a difficult analytical problem. Numerical results from ORACLE are easier to obtain. Figure 10 shows a single realization of the irradiance spectrum as a function of $\kappa_y(\kappa_x=0)$ for a linear velocity profile in the y direction. The spectrum for this case is a function of the full wave vector κ. Its growth is strongly suppressed for wave vectors parallel to the shear for $S=0.886$ and 1.77. Though not shown, the spectrum for $\kappa_y=0$ is unaffected by the shear. In practice, for a given S there exists a critical rate of blooming below which STRS growth is suppressed. This critical value changes with different velocity profiles and must be determined empirically. Equivalently, for a specific family of velocity profiles parameterized by S, there exists a critical value of S above which STRS growth is suppressed for a fixed irradiance. For the previous case of a 1-μm beam propagating 1 km with a blooming rate of 10 waves per second, the shear ratio given $\Delta v=1$ m/s is $S=2.8$.

CONCLUSION

The linearized theory of small perturbations in thermal blooming gives a surprisingly accurate description of the initial evolution of a beam propagating through an absorbing medium. For the case in which the absorption and velocity of the medium are constants, the theory is analytically tractable and correctly predicts the growth rates of perturbations. A sinusoidal perturbation of the optical field grows exponentially at a rate determined by its Fresnel number and the accumulated optical-path difference (OPD) due to blooming. The growth rate for

perturbations with very small length scales reduces to a function of the accumulated OPD only. More complicated cases with varying absorption and velocity profiles can be analyzed using a WKB approximation. Numerical simulation of a linear velocity profile shows suppression of the growth rates governed by the magnitude of the nondimensional shear.

The evolution of optical turbulence in the medium is also correctly predicted by the linear theory, as well as the evolution of the Strehl ratio. The optical turbulence appears as an initial condition and does not affect the evolution of the spectrum to first order. The initial damping of the large-scale turbulence leads to a small increase in the Strehl. However, the small-scale turbulence fluctuations always grow and are eventually joined by large-scale fluctuations leading to a rapid drop in Strehl. The spectrum eventually saturates when the nonlinearity of the full system becomes important. However, up to saturation the predictions from linear theory agree well with results from numerical simulations of the full nonlinear system and thus provides a benchmark of comparison between different numerical codes. Finally, the growth of small-scale perturbations limits the amount of power a laser can transmit coherently through a turbulent medium such as the atmosphere. This holds even for propagation using adaptive optics correction schemes, which can correct only larger scale distortions.

ACKNOWLEDGMENTS

The authors would like to acknowledge Keith Brueckner, Marshall Rosenbluth, William Dannevik, James Davis, and Brian Hatfield for stimulating conversations regarding this subject. This research was performed jointly under the auspices of the U.S. Department of Energy by Lawrence Livermore National Laboratory under Contract No. W-7405-ENG-48 for the U.S. Army in support of funding order W31RPD-7-D4041.

APPENDIX: DERIVATION OF UPPER BOUND FOR $K(z,t)$

The steps used to obtain the upper bound [Eq. (14)] for the blooming function $K(z,t)$ are briefly outlined here. The first step is to write $K(z,t)$ in terms of the Bessel functions $J_0(x)$ and $I_0(x)$:

$$K(z,t)=zh(\xi,\eta)/\sqrt{\xi}\ , \tag{A1}$$

$$h(\xi,\eta)=\int_0^{\xi} f'(x)J_0(\sqrt{\eta(\xi-x)})dx\ , \tag{A2}$$

$$f(x)=2^{5/6}x^{1/3}\mathrm{Re}\left[e^{i\pi/6}\int_{-\infty}^{\infty} e^{-\zeta y^4}I_0(\zeta y)dy\right]\ , \tag{A3}$$

$$\zeta=4(2x)^{1/3}e^{-i\pi/3}\ ,$$

where $\xi=\Gamma t a_\kappa k z^2$, $\eta=a_\kappa/\Gamma t k$, and $f'(\xi)=df/d\xi$. An upper bound for f' can be calculated using the upper bound for I_0, $|I_0(\zeta|r|)|\le\exp(\beta|r|)/\sqrt{\beta|r|}$, $\beta=\mathrm{Re}(\zeta)$:

$$|f'(x)|\le\frac{e^{3x^{1/3}/2^{4/3}}}{(2x)^{5/6}}\int_0^{\infty} e^{-y_0^2\beta(y-y_0)^2}(1-2\beta y)\frac{dy}{\sqrt{y}}\ ,$$

$$y_0=1/2^{2/3}\ . \tag{A4}$$

For $1\le x\le\xi$, the integral is split into an integral over the range 0 to $y_0/2$ and an integral over the range $y_0/2$ to ∞. An upper bound is calculated for each integral separately and combined to obtain

$$|f'(x)|\le\frac{a}{x^{2/3}}e^{3x^{1/3}/2^{4/3}}+\frac{c\xi^{1/2}}{x^{2/3}}e^{9x^{1/3}/2^{10/3}}\ , \tag{A5}$$

where $a=(2^{5/3}+1)\sqrt{\pi/3}$ and $c=\frac{7}{6}+(\frac{1}{2})^{2/3}$. A series expansion for $f'(x)$ gives an upper bound in the range $0\le x<1$:

$$|f'(x)|\le\frac{1}{2\sqrt{x}}\ . \tag{A6}$$

From these results, an upper bound for $h(\xi,\eta)$ for $\xi>1$ can be calculated:

$$\begin{aligned}|h(\xi,\eta)|&\le\int_0^{\xi}|f'(x)|dx\\&\le 1+\int_1^{\xi}(ae^{3x^{1/3}/2^{4/3}}\\&\qquad+c\xi^{1/2}e^{9x^{1/3}/2^{10/3}})\frac{dx}{x^{2/3}}\\&\le 1+22.1\xi^{1/6}e^{3\xi^{1/3}/2^{4/3}}\ ,\end{aligned} \tag{A7}$$

where

$$22.1=2^{4/3}(a+\tfrac{8}{3}ce^{-3/2^{10/3}})\ .$$

The bound for $K(z,t)$ is obtained from (A7):

$$\begin{aligned}|K(z,t)|&=z|h(\xi,\eta)|/\sqrt{\xi}\\&\le\frac{22.4z}{\xi^{1/3}}e^{3\xi^{1/3}/2^{4/3}}\ ,\end{aligned} \tag{A8}$$

where $22.4 = 22.1 + \exp(-3/2^{4/3})$. The upper bound in the text, Eq. (14), can be obtained from (A8) by using the identity $\xi=\pi^3N_\lambda/2N_p$.

[1]J. L. Walsh and P. B. Ulrich, in *Laser Beam Propagation in the Atmosphere*, edited by J. W. Strohbehn (Springer-Verlag, New York, 1978).

[2]A. K. Gautesen and J. R. Morris, Lawrence Livermore National Laboratory Technical Report No. UCID-21501 (unpublished).

[3]N. M. Kroll and P. L. Kelley, Phys. Rev. A **4**, 763 (1971).

[4]T. J. Karr, M. C. Rushford, J. R. Murray, and M. R. Morris, Lawrence Livermore National Laboratory Technical Report No. UCRL-99967 (unpublished).

[5]K. A. Brueckner and S. Jorna, Phys. Rev. **164**, 182 (1967).

[6]V. V. Vorob'ev and V. V. Shemetov, Izv. Vyssh. Uchebn. Zaved. Radiofiz. **21**, 1610 (1978).

[7]K. S. Gochelashvili, I. V. Chasei, and V. I. Shishov, Sov. J. Quantum Electron. **10**, 1207 (1980).

[8]V. S. Averbakh, A. A. Betin, V. A. Gaponov, A. I. Makarov,

G. A. Pasmanik, and V. I. Talanov, Izv. Vyssh. Uchebn. Zaved. Radiofiz. **21**, 1077 (1978).

[9]R. J. Briggs, Lawrence Livermore National Laboratory Technical Report No. UCID-21118 (unpublished).

[10]T. J. Karr, J. Opt. Soc. Am. A **6**, 1038 (1989); Lawrence Livermore National Laboratory Technical Report No. UCID-21172 (unpublished).

[11]J. R. Morris, M. Opt. Soc. Am. A **6**, 1859 (1989); Lawrence Livermore National Laboratory Technical Report No. UCID-21261 (unpublished).

[12]A. J. Glass (private communication).

[13]J. Viecelli, Lawrence Livermore National Laboratory Technical Report No. UCID-21589 (unpublished).

[14]J. A. Fleck, J. R. Morris, and M. D. Feit, Appl. Phys. **10**, 129 (1976).

[15]V. I. Tatarski, *Wave Propagation in a Turbulent Medium* (Dover, New York, 1961).

[16]The first few terms of this series were derived independently by B. Hatfield, North East Research Associates, Woburn, MA (Private communication).

[17]D. L. Fried, J. Opt. Soc. Am. **56**, 1372 (1966).

[18]H. T. Yura, Appl. Opt. **11**, 1399 (1972).